Construction and Building Materials 49 (2013) 407–416

Contents lists available at ScienceDirect

Construction and Building Materials

journal homepage: www.elsevier.com/locate/conbuildmat

Pore structure in concrete exposed to acid deposit

FAN Ying-fang *, LUAN Hai-yang

Institute of Road and Bridge Engineering, Dalian Maritime University, Dalian 116026, China

HIGHLIGHTS

- Development of pore structure in concrete exposed to acid deposit is studied.
- The pore structures of interior concrete are determined by using MIP, SEM, and CT.
- The probabilistic distribution model is suggested for porosity of the concrete under various exposure conditions.
- Relation between porosity and the mass change is analyzed.

ARTICLE INFO

Article history:
Received 26 March 2013
Received in revised form 15 August 2013
Accepted 29 August 2013
Available online 20 September 2013

Keywords:
Concrete
Acid deposit
Porosity
Multiscale
SEM
MIP
CT

ABSTRACT

Pore structure has a significant effect on the mechanical response and durability of concrete. To well understand damage evolution of concrete exposed to the acid deposit, the pore characteristics inside the concrete were studied from multi-scale levels. To simulate the acid deposit, acid solutions with pH level of 1.0, 1.5 and 2.5 were deposed by the mixture the sulfate and nitric acid in the laboratory. The pore structures of concrete under various deterioration states were examined by mercury intrusion porosimetry (MIP) test and scanning electron microscopy (SEM). Contents of the chemical elements in the concrete samples were measured by Energy Dispersive Spectra (EDS) analysis. Computed tomography (CT) test was carried out to examine the meso-structure in concrete at the desired exposure ages. The CT digital images were processed and analyzed by Pro-Plus software. According to the probabilistic analysis of the porosity, it is indicated that the porosity in all the concrete specimens under various damage conditions obeys to the normal distribution. A distribution density function of the porosity in concrete specimens was suggested, and it was revealed that the mean and variance values of the porosity decrease linearly with the conditioning age. It was illustrated that the porosity has a slight increase at the initial exposure period, and decreases gradually with the elongation of the conditioning age. The higher acidity of the conditioning environment was, the more obvious changes of the porosity in concrete occurred. The evolutions of pore character are discussed from both the micro- and meso- levels, which can well discover the development mechanism of macro- behavior of concrete exposed to acidic environment.

1. Introduction

Durability of concrete structures in aggressive environments has become a major concern to the scientific community over the past several decades. At the present time, early age deterioration of the world's infrastructure is motivating the understanding of deterioration process of the construction materials. Some work has been done to investigate the mechanical performance of concrete in severe environment, and knowledge has been obtained [1–4]. However, the performance of the concrete (such as permeability, mechanical behavior, and durability.) is critically affected by the characteristics of the pore structure. The intensity of the interactions with the aggressive agents, and external loads always lead to the change of the pore structure inside concrete [5]. The results revealed that the change in micro structure, chemical content and pore structure are the critical reasons resulting in the deterioration of mechanical behavior of concrete. In order to discover the deterioration process of concrete servicing in the acidic environment, the understanding of the pore characteristics inside the concrete under various damage states is a crucial step.

Many research studies have been examined the microstructure of cementations materials [6–11]. Zhang carried out experiments on the effect of curing on the degree of capillary porosity of concrete in a tropical environment [12]. Duan studied the pore structure of concrete incorporating metakaolin (MK) when exposed to two types of curing conditions, seawater and fresh water. The results showed that the seawater curing condition further causes a corresponding low porosity at early days and a corresponding high porosity at later days [13]. Mendes' study indicated that a higher

* Corresponding author. Tel.: +86 13998546368.
E-mail address: fanyf72@yahoo.com.cn (Y.-f. FAN).

0950-0618/$ - see front matter © 2013 Elsevier Ltd. All rights reserved.
http://dx.doi.org/10.1016/j.conbuildmat.2013.08.075

Table 1
Mix proportion of the concrete.

Cement (kg/m^3)	Sand (kg/m^3)	Coarse aggregate (kg/m^3)	Water (kg/m^3)	w/c	w/b	Undisturbed fly (ash/kg)	Reducing-water (agent/kg)	Slump (mm)
450	678	1040	159	0.353	0.304	60.0	12.8	180

Table 2
Conditioning details.

Series	Specimen dimension (mm)	Solution acidity	Immersion time (days)
CA-1	10 × 10 × 10	pH1.0	0,3,7,10
CA-2	10 × 10 × 10	pH1.5	0,3,7,10
CA-3	10 × 10 × 10	pH2.5	0,3,7,10
CB-1	150 × 150 × 150	pH1.5	0,5,10,15,20,30,40
CB-2	150 × 150 × 150	pH2.5	0,5,10,15,20,30,40

porosity and coarser capillary pore size distribution (PSD) in paste compared to paste in concrete [14]. Chen conducted an experimental study to evaluate the effect of curing conditions on the porosity of concretes made with high slag blast furnace cement (HBFC) and ordinary Portland cement (OPC) [15]. Up to now, few studies considered the development of pore character in concrete with the action of acid deposit. Few results about the porosity distribution character in concrete suffering various damage conditions were reported.

The main objective of this study was to investigate the pore structures of concrete exposed to acid deposit from multiscale levels. The acid solutions with pH level of 1.0, 1.5 and 2.5 deposed by the mixture the sulfate and nitric acid in the laboratory were considered. After being exposed to the acidic solution for the desired periods, the concrete samples were picked out. The removed specimens were first dried for about two to three days, followed by the physical, computed tomography (CT), and scanning electron microscopy (SEM)/energy dispersive spectra (EDS) test. The CT digital images were processed and analyzed by Pro-Plus software. The threshold value is suggested for the identification of the pore. The developments of pore structure and porosity inside the concrete samples are examined. Pore distribution and porosity of concrete specimens suffering various deterioration processes are obtained. The relation between the pore characteristic and physical performance of concrete are discussed.

2. Experimental programme

2.1. Specimen preparation

Mix proportion of the concrete mixtures is shown in Table 1. The concrete mix was proportioned using the procedure recommended in the present code [16]. Cubic specimens with the dimension of 150 mm × 150 mm × 150 mm were cast. After being demoded after 24 h, the specimens were stored in the curing room for 28 days. Then, the compressive strength was tested according to the procedure recommended in the current standard [17]. The tested 28-day compressive strength of the designed concrete is 40 MPa. In order to obtain the pore distribution in concrete from micro-level, 10 mm × 10 mm × 10 mm cubic samples were drilled from the specimen.

2.2. Accelerated corrosion procedure

Two types of tests are usually used to simulate concrete structures attacked by environmental conditions: site and accelerated corrosion tests [2]. Although long-term exposure site test [18] can best simulate field conditions, it takes much longer time to achieve desired deterioration. Therefore, accelerated corrosion test was used in most of the past studies and is also adopted herein.

Submerging and spraying are the two main ways to accelerate concrete deterioration caused by acid rain in the laboratory. Based on the previous study [2,3], although the two methods are comparable and both give reliable results, the submerging method is more suitable for cement concrete, and is therefore adopted for accelerated ageing in this study. Since the acid rain is due to sulfuric acid in most parts of China, sulfuric acid type acid rain is simulated in this study. Acidic solutions with pH level of 1.0, 1.5 and 2.5 were deposed by the mixture of sulfate and nitric acid solutions (molar ratio is 9:1) in the laboratory, respectively. Acidity of the solution was recorded by PB-10 sartorius acidometer. The pH levels of the acid solutions were detected by the digital pH meter [19]. To keep the pH level of the mixed solution constant, nitric acid solution was added periodically. At the same time, the solution was stirred thoroughly to reduce differential concentrations of the acid inside the solution container. The specimens were divided into four groups denoted by series CA-1, series CA-2, series CA-3, series CB-1 and CB-2 (Table 2). Series CA is the 10 mm × 10 mm × 10 mm cubic samples, and Series CB is the 150 mm × 150 mm × 150 mm cubic specimens. Series CA-1 through CA-3 was conditioned in solutions with pH levels of 1.0, 1.5 and 2.5, which covers practical range of the acidity of acid rain worldwide (Fig. 1). Series CB-1 and CB-2 were conditioned in solutions with pH levels of 1.5 and 2.5 respectively. Ageing effects were taken into consideration for all groups.

After being exposed to the acidic solution for the desired periods listed in Fig. 2, the samples were picked out. The removed specimens were firstly dried for about two to three days, followed by the physical, CT and SEM/EDS test.

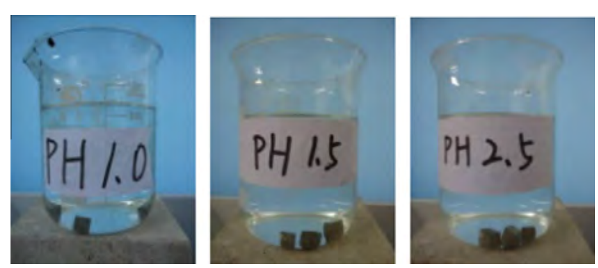

Fig. 1. Concrete specimens exposed to the acid rain solution with various pH levels.

Fig. 2. 16 slice spiral CT scanner.

2.3. Multi-level investigation of pore character inside the specimen

2.3.1. Mercury intrusion porosimetry (MIP)

Water vapor adsorption and nitrogen adsorption test, mercury intrusion porosimetry (MIP) test are the most popular methods used to examine the pore characteristics inside concrete [20]. Ultrasonic, as a kind of nondestructive technique, has been used to assess porosity inside concrete [21,22]. But the research reports that it is quite difficult to obtain precise evaluations of the ultrasonic parameters. Mercury intrusion porosimetry is a technique that is known to present some limitations in obtaining an accurate measurement of the pore size distribution of hydrated cements [23]. However, it is widely used to characterize cementitious materials, provides valuable information about threshold diameters and intrudable pore space, and is applied in this research to obtain semi quantitative information regarding pore structure and connectivity for hydrated blends of cementations materials.

In this study, the pore size distributions in concrete under various exposure conditions were measured by MIP. The instrument used was AutoPore II 9220 with an intrusion pressure between 13,782 Pa and 227.4 MPa, manufactured by Micromeritics Instrument Corporation.

2.3.2. Scanning electron microscopy (SEM)

SEM is a well-established method that can offer useful information concerning the structural material (Rendell, 2002). To better understand the evolution of microstructure of the concrete samples exposed to acidic solution with desired ages (0 day, 3 days, 7 days and 10 days), micro-structure of the samples were observed by JSM-6360LV SEM system. The applied voltage and intensity is 20 kV. Energy dispersive spectroscopy (EDS) technique was applied to analyze the elemental distribution in the samples as well. The EDS plots provide the presence of the chemical elements, which will confirm the composition of crystal in the concrete samples. To make the samples conductive, the surface of the samples was coated with 10 nm thick gold.

2.3.3. Computer tomography (CT)

Since the X-rays are absorbed by the concrete specimen according to the composition and density of the material, different features can be detected. Objects with a higher density absorb more X-rays, resulting in bright areas. Consequently, the lower the density is, the less X-rays are absorbed, creating darker regions. That means the pores appear very dark. Accordingly, the pores can be distinguished and quantified by image analysis of the 2-D sections. In this research, CT technology was selected to describe the porosity character of concrete specimen under various deterioration states.

For the measurements, a 'Siemens somatom sensation' 16-slice spiral computed tomography scanner made in Germany was used. Samples were scanned with a fixed X-ray source, at 140 kV, 200 mA and 22.60 mGy CTD. Each scan was 1 mm thick and the total number of the scans was about 200.

3. Results and discussions

3.1. Micro level analysis

3.1.1. Evaluation of the pore structure in concrete

The pore size distributions in concrete of all three samples, which are denoted as A1, A2 and A3 were measured. The pore size distribution curves of concrete samples are presented in Fig. 3 and Table 3. According to the pore size, pores are classified into harmless pore, less harm pore, harmful pore and more harm pore (shown in Table. 4).

The pore size distributions in the concrete samples (Fig. 3) show that the average porosity is 17.96%, and the average pore diameter is 47.3 nm. The pores smaller than 50 nm are occupied around 70% of the total pores. The more harm pore occupied nearly 4% of the total pores. Therefore, most of the pores in the concrete tested in this paper have little harmful effect on its performance in the normal conditions.

3.1.2. Scanning electron microscopy (SEM)

SEM micrographs of concrete samples at different exposure periods are achieved, which are shown in Fig. 4. The development of cracks in the concrete samples exposed to the acid solution is shown in Fig. 5 as well.

From the SEM images, it is obvious that progressive and significant alternation occurs in the internal microstructures of concrete samples during the exposure periods. With the development of exposure age, the C–S–H becomes denser and smoother, more and more AFt and C–H crystal are formed, the internal pore diameter becomes wider, and the micro cracks in the samples become wider and longer. What is more, the morphology of internal microstructure in the samples becomes softening with the prolongation of the exposure age.

3.1.3. EDS analysis

Owing to the chemical reactions between the acid solution and concrete, the compositions in the concrete are changed. To clarify the composition of products generated by acid attack, EDS were carried out on the surface of products shown in SEM micrograph.

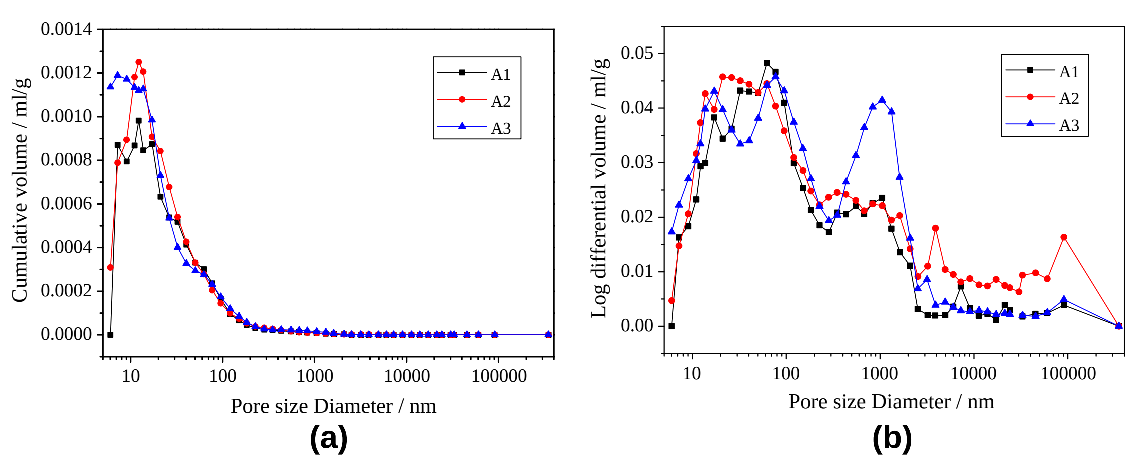

Fig. 3. Variations of cumulative intrusion for concrete samples.

Table 3
Porosity characteristic of the controlled concrete samples.

No	Total intrusion (volume/ml g^{-1})	Total pore area (m^2 g^{-1})	Median pore diameter (volume/nm)	Median pore diameter (area/nm)	Average pore (diameter/g ml^{-1})	Bulk density at 0.52 (psia/g ml^{-1})	Porosity (%)	Average pore size (diameter/nm)
A1	0.0771	6.729	90.4	19.1	2.4198	2.0393	15.7247	45.8
A2	0.1016	7.841	159.5	17.9	2.3874	1.9214	19.5213	51.8
A3	0.0949	8.582	128.5	15.3	2.4139	1.9639	18.6412	44.2
Mean	0.0912	7.717	126.1	17.43	2.4070	1.9749	17.9624	47.3

Table 4
Porosity size distribution of concrete samples.

No.	Pore content/ %				Total specific pore (volume/ml g^{-1})	<50 nm (%)
	<20 (nm)	20–50 (nm)	50–200 (nm)	>200 (nm)		
A1	30.7	35.5	30.0	3.8	0.000982	66.2
A2	28.6	43.9	23.6	3.9	0.001206	72.5
A3	33.2%	40.4	22.3	4.1	0.001136	73.6

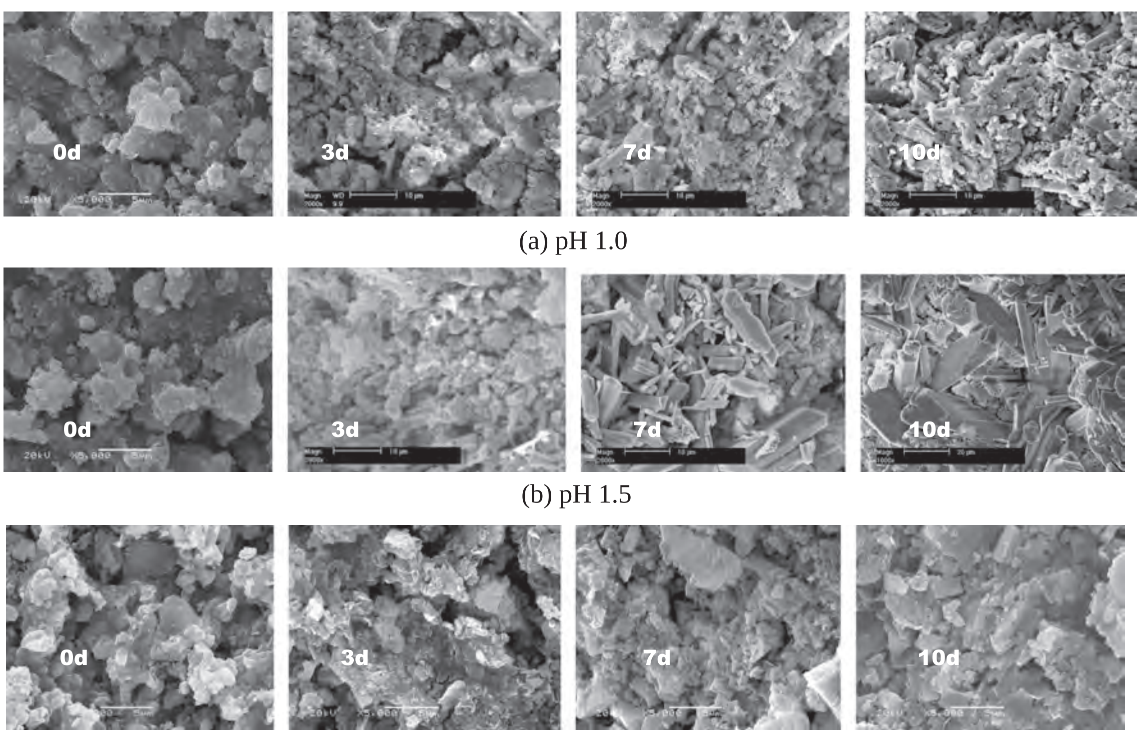

Fig. 4. The change of concrete samples surface structure.

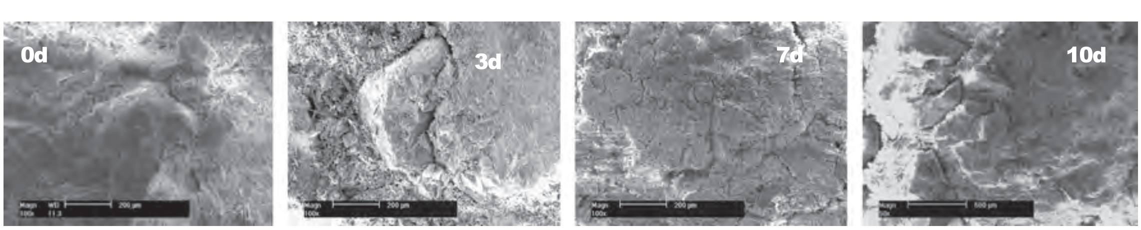

Fig. 5. Typical crack of concrete surface.

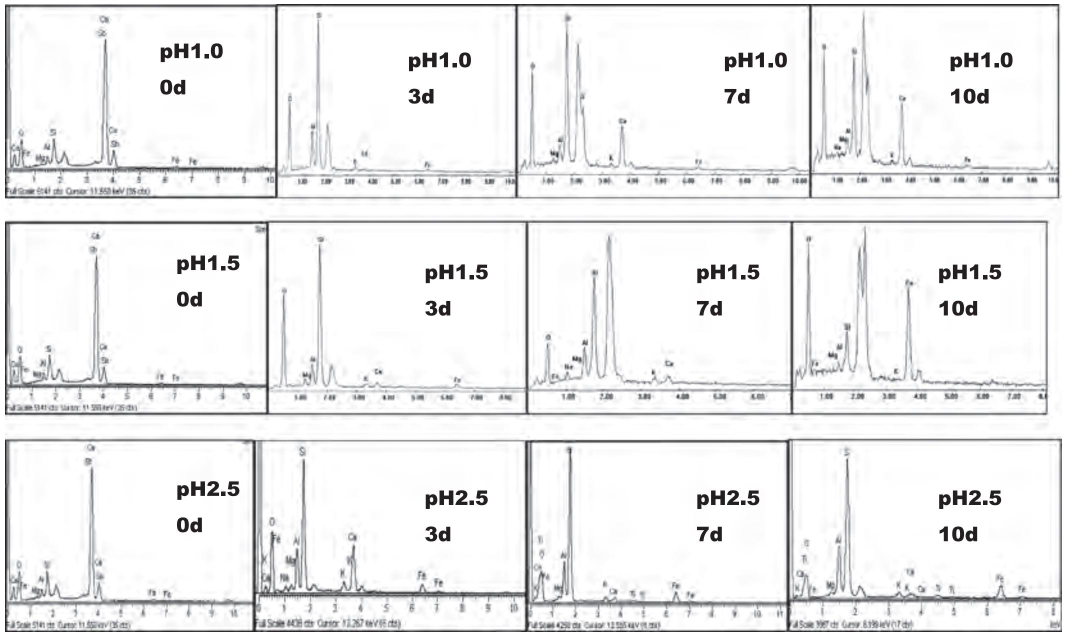

Fig. 6. EDS spectra for concrete specimen. *Note*: the *X*-axis is energy (keV), the *Y*-axis is the element strength.

EDS plots show the presence of calcium, silicon, aluminum, oxygen, magnesium, ferrum, kalium. The principal elements are calcium, silicon, aluminum and oxygen. From EDS test, an indication of the number of atoms in the species being examined is obtained as well. The number of elemental and atomics distribution in concrete samples at various exposure ages are counted and percentages are ascribed respectively, which are plotted in Fig. 6.

From Fig. 6, it is clear that the content of Calcium has a significant reduction and the content of Silicon has an obvious increase in the samples exposed to acid solution. This result is in good agreement with the interpretation of deteriorating mechanism of concrete in acid medium reported by other researches [24–26]. That is, more soluble products are formed through the chemical reaction between the cement and nitric acid, sulfate acid and calcium hydroxide. Therefore, calcium compounds of cement paste formed in concrete through the hydration process and the calcium in calcareous aggregate are leached away, and silica gel or sometimes magnesium silicate hydrate fill the space. As a result, the strength and durability will decrease gradually.

3.2. Meso-level analysis

After curing the concrete prism specimen in water for 28 days, it was taken out and scanned. Each scan was 1 mm thick, and the total number of the scans was about 150. The internal meso-level structure of the specimen is specified based on the 150 scanning images. Then, the specimens were conditioned in the simulated acid solution for further corrosion and scanned again at the desired time.

3.2.1. CT digital image

The output scanning section of concrete is recorded by the document of DCM format, and the CT number is stored in 12 digital capacities. As a result, each pixel can display 4096°. The output digital image is 512 × 512 pixel points (shown in Fig. 7).

From Fig. 7, it is clear that for the specimen conditioning in the acid solution with pH level of 1.5, the void in the specimen become bigger, and the darker regions become wider. However, for the specimen conditioning in the acid solution with pH level of 2.5, the void in the specimen gets slightly smaller in the initial 10 days, with the conditioning continues, the void in the specimen become bigger. That is, the density of concrete specimen becomes lower with corrosion continues. The result is in good agreement with the visual observation of specimen, which more and more honeycomb voids are formed with the corrosion continues.

3.2.2. Image processing

To clarify the objective region and the background, the image edge detection was performed on the CT images. Five kinds of

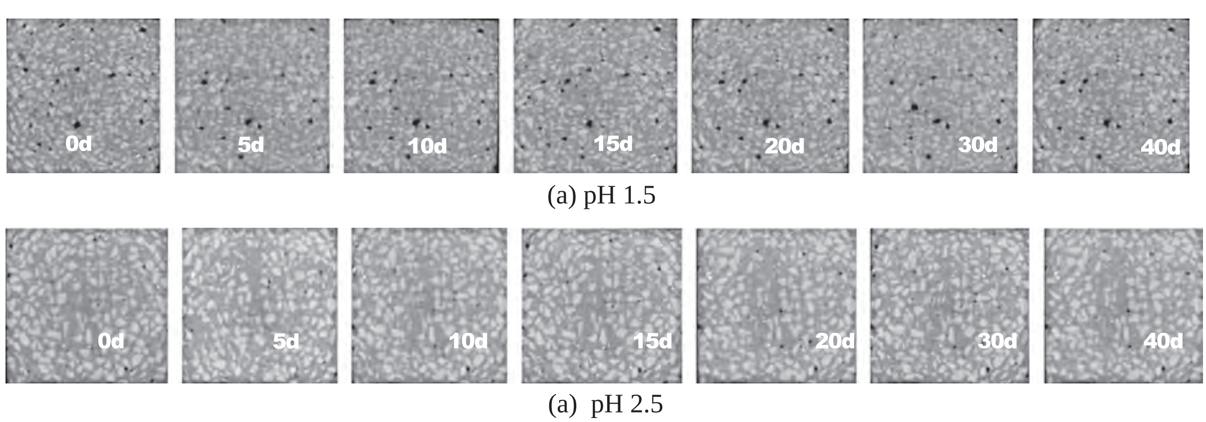

Fig. 7. CT scanning images of concrete specimen conditioning in acidic solutions.

Fig. 8. The contrast of edge detection.

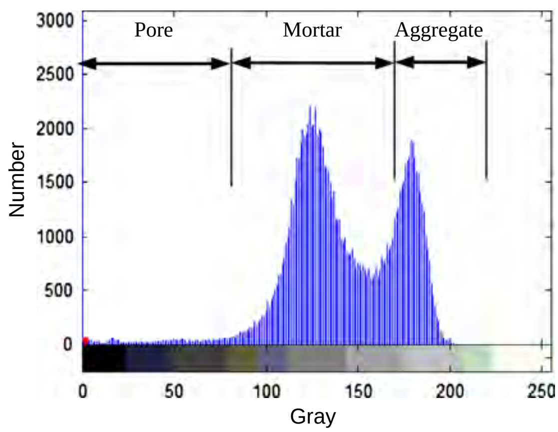

Fig. 9. Gray-level histogram.

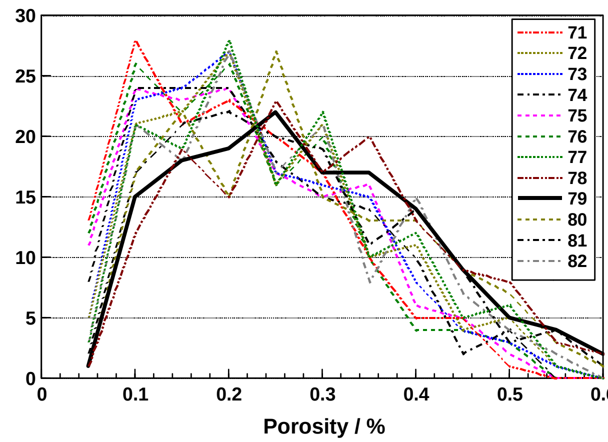

Fig. 11. Porosity statistical figure of different gray threshold.

operators, which inclusive of roberts operator, prewitt operator, sobel operator, log operator and canny operator, were applied for the image edge detection of CT digital sections. The identified images obtained by the above five operators are shown in Fig. 8.

Comparing the recognition effects of the five operators, it is shown that the canny operator is the most effective operator for identifying the interfacial transition zone (ITZ) between aggregates and hydrated paste.

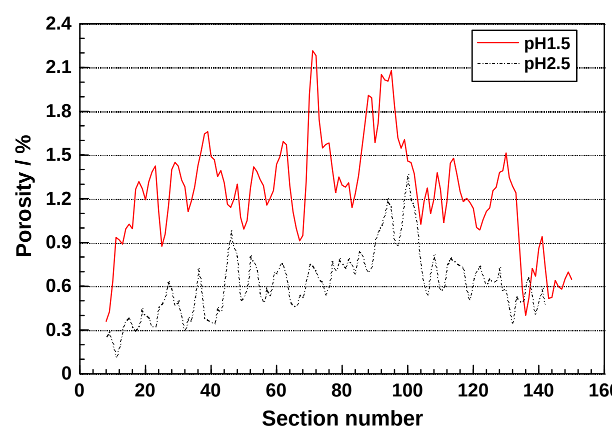

Fig. 12. Porosity distribution of concrete samples.

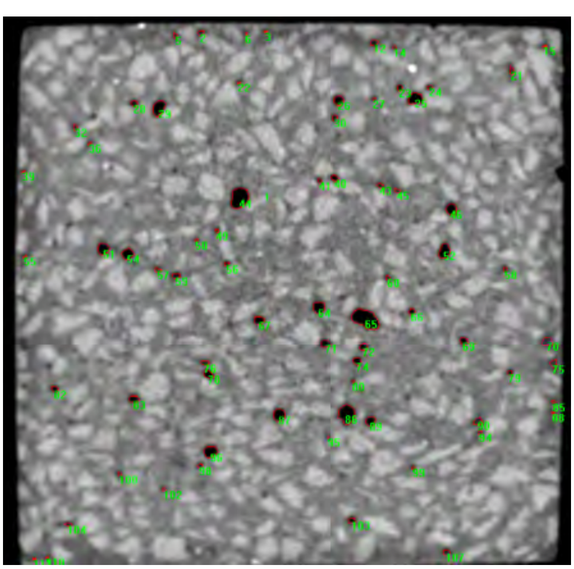

Fig. 10. Pore distribution recognition.

3.2.3. Determination of the threshold value for identifying the pore structure

To identify the pore distribution inside the concrete specimen, binary processing was executed on the scanning digital images. The binary processing function was expressed as:

$$g(x,y) = \begin{cases} 0 & f(x,y) \leqslant T \\ 255 & f(x,y) > T \end{cases} \tag{1}$$

where $f(x, y)$ is the gray value of the pixel point (x, y); and T is the pore grayscale threshold.

According to the theory of gray-level image thresholding method, a threshold should be determined firstly. Then, the gray scale values of each pixel are compared with the given threshold. Once the gray scale value on the pixel point is bigger than the threshold,

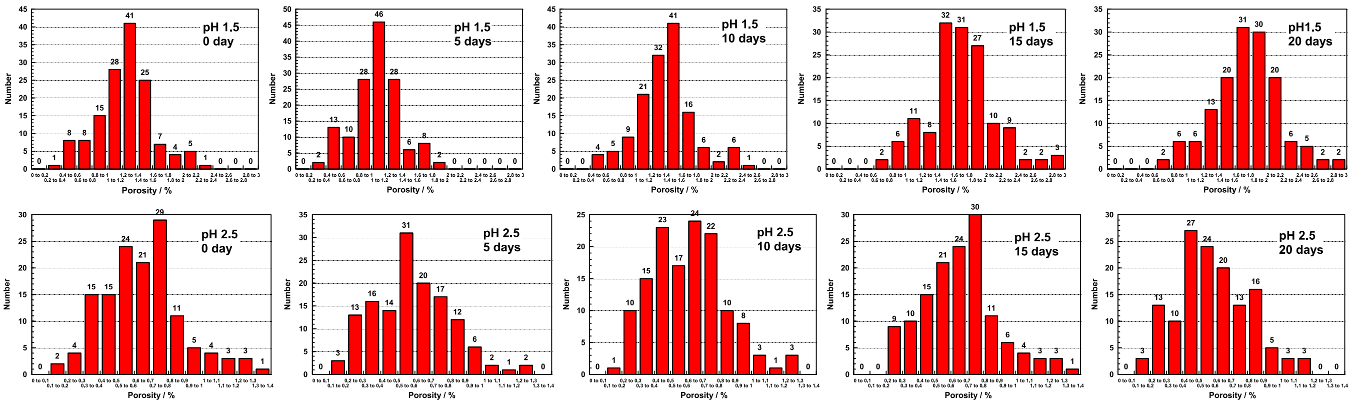

Fig. 13. Probability distribution of the porosity inside concrete specimens.

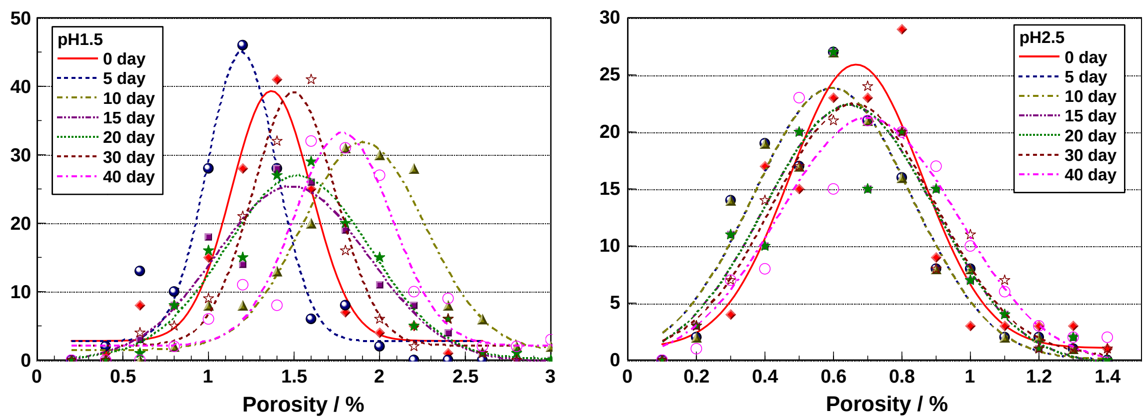

Fig. 14. Probabilistic analysis of the porosity in the concrete samples conditioning in the acidic solutions.

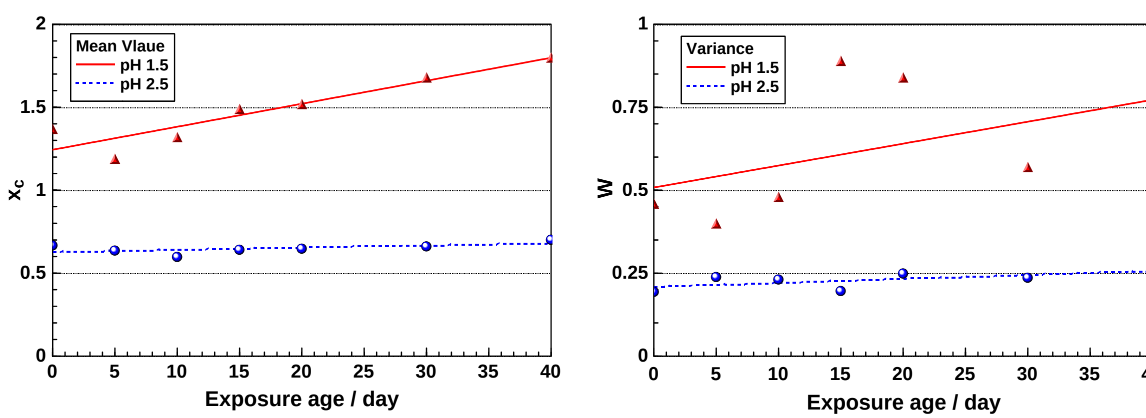

Fig. 15. Relation between the parameters of Gaussian distribution function with exposure age.

the gray scale value on this pixel point is 255. Otherwise, the gray scale value on this pixel point is zero. Therefore, the primary problem is to determine a reasonable threshold. In this research, image segmentation technology was applied for determining the threshold. Gray histogram of the scanning images was obtained by Matlab software, which is given in Fig. 9.

From Fig. 9, it can be seen that double peaks appear in the graph. The objective and background can be divided into two parts by the gray scale value at the valley bottom. It can be derived that the range of the threshold value is between 70 and 82. The internal pores in the concrete specimen were recognized by the Pro-Plus software. The obtained pore-recognition graph for one section is plotted in Fig. 10. Assuming that threshold value is between 70 and 82, porosity for each section can be calculated (Fig. 11).

From Fig. 11, it can be concluded that 79 is the optimal threshold value for the identification of the pore inside the concrete.

3.2.4. Development of porosity inside concrete

Using the obtained optimal threshold value, the digital images were processed by a programming calculation with Pro-Plus. The identification of pore inside the concrete was realized. Pore recognition graph of the concrete specimens under various damage states was then arrived at, and the porosity of the sections were computed. The corresponding porosity of 120 2-D sections images

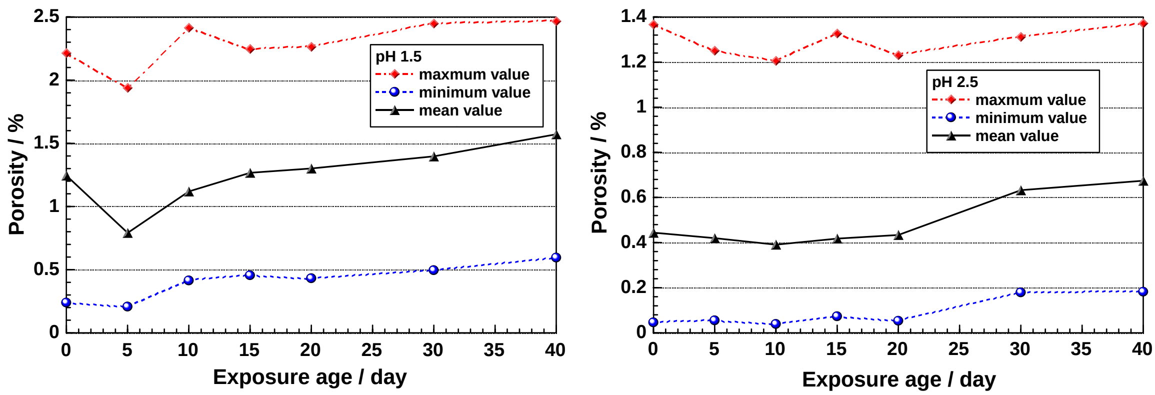

Fig. 16. Relation between porosity and exposure age.

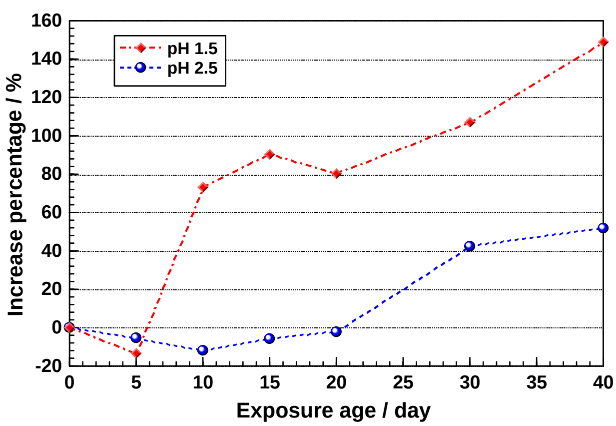

Fig. 17. Development of porosity along with exposure age.

for each concrete specimen under various exposure conditions are obtained respectively (shown in Fig. 12).

From Fig. 12, it is clear that the porosity distribution in the concrete samples fluctuate up and down in the 120 2-D section images. Based on the theory of probabilistic statistics, the probabilistic characteristics of porosity distribution inside the concrete specimens were studied furthermore. The analysis results of the porosity characteristics inside the concrete specimens under various exposure conditions are shown in Fig. 13 respectively.

From Fig. 13, it is obvious that the distribution of the porosity inside the concrete specimens obeys the normal distribution. Development of the average porosity inside concrete specimen conditioned in the acidic solutions along with the conditioning age is given in Fig. 14.

Therefore, the distribution density function of the porosity in concrete specimens can be expressed as:

$$p(\rho) = \frac{1}{\sqrt{2\pi}} e^{-\frac{(x-\mu)^2}{2\sigma^2}} (0 < \rho < \infty) \quad (2)$$

where ρ is the porosity in concrete specimen, μ and σ are the mean value and variance of the Gaussian distribution. Fig. 15 shows the relation between the parameters of Gaussian distribution function and exposure age. The maximum value, minimum value and the average value of porosity in the concrete specimens are obtained (Fig. 16). Moreover, the influence of acid solution on porosity development along with the exposure age is shown in Fig. 17.

Overall, it is evident that the porosity of specimens exposed to the acid solution with pH level of 1.5 decreased 13.4% of the controlled specimen in the initial five days, followed by the increase in the later ages. The porosity has increased 149% of the controlled specimen for specimens immersed in acid solutions with pH level of 1.5 for 40 days. On the other hand, the porosity of specimen in the acid solution with pH level of 2.5 showed higher porosity up to 20 days, followed by the decrease in the later ages. The porosity has decreased 11.9% of the controlled specimen for 10 days, and the porosity decreased 51.8% after exposing for 40 days. The effect of the acid solution creates a more porous concrete microstructure in the concrete. The development of the porosity shows a good agreement with the results provided by the mass, strength analysis from macro-level test (shown in Fig. 3).

3.3. Macro-level analysis

3.3.1. Visual observation

From visual inspection of the samples exposure to acid solution for various exposure periods (shown in Fig. 17), it can be seen that the surface become to be yellow and the surface dissolution of cement paste lead to exposure of aggregates.

From Fig. 18, it is observed that as conditioning continued, surface color gradually changed from gray to gray-black, and then yellow, and finally yellow–brown. Honeycomb voids were formed and coarse aggregates were exposed in the very outer skin of the concrete. Damage initiated from the prism corners, and the specimens became loose and powdery. The deterioration was more significant for specimens conditioned in the solution with higher acidity, which is similar to what observed by Xie and Fan ([2,27]).

3.3.2. Mass change

Based on the visual observations mentioned above, it was obvious that honeycomb voids were formed as conditioning continued, causing the mass change. This could be measured by an electronic scale with an accuracy of 0.1 g. Relation between the mass change and conditioning age is given in Fig. 18(a). Based on the theory of meso-mechanics, concrete can be considered as a combined material which is consisted of base material and void. Relation between the volume of base material and voids can be expressed as [28],

$$C_1 = (m_{t0} - m_{tt})/m_{tt}, \quad C_1 + C_0 = 1 \quad (3)$$

Where, m_{tt} is the mass of concrete specimens immersed in the acid solution for t days; m_{t0} is the mass of undamaged concrete specimens; C_1 is the volume of voids, and C_0 is the volume of base material. In this way, the relation between the developments of voids volume over time can be obtained quantitatively, which is shown in Fig. 18(b).

Fig. 19 shows that the mass of the specimen have a slight increase at the initial five days, but decreases with the conditioning age later on. The result keep in good agreement with the results

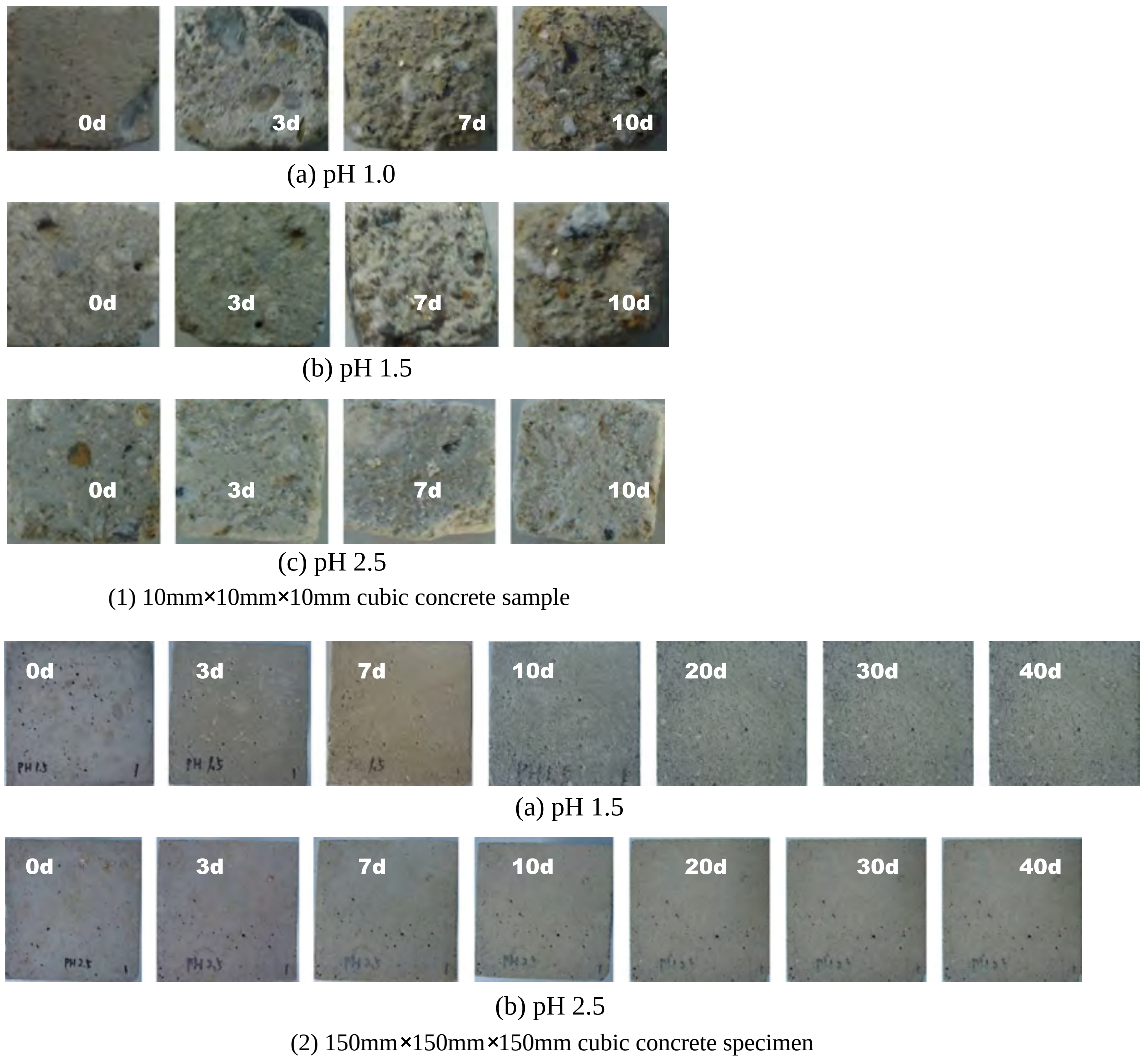

Fig. 18. Surface of concrete samples exposed to acidic solution. (a) Relation between the mass change and conditioning age and (b) relation between C_1 and conditioning age.

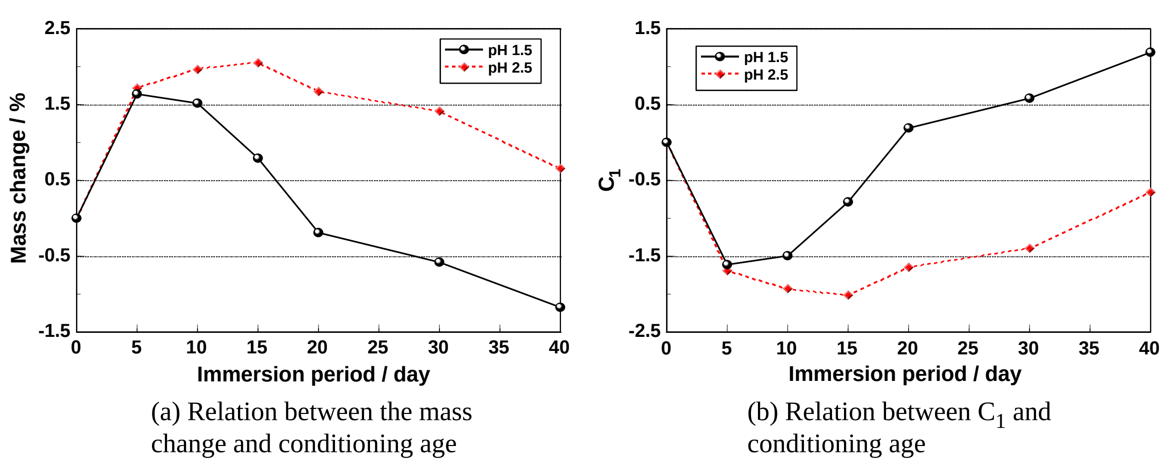

Fig. 19. Relation between void volume and immersion time.

obtained from the above meso-level analysis (shown in Fig. 14). That is, in the initial conditioning age, the porosity in the concrete decreases which results in the mass increase. However, with the conditioning continues the porosity in the concrete increases and leads to the mass decrease.

4. Conclusions

This paper assesses the development of pore structure in concrete exposed to the acidic environment from multiscale levels. A series of tests, including physical tests, MIP, CT, SEM/EDS were performed on the concrete specimen under various conditioning states. Mass loss, voids property, meso and micro pore structure in the concrete specimens under various damage states were examined quantitatively. The results obtained on different scales are compared and discussed in detail. The conclusions from this study are summarized as follows:

(1) CT technology provides a useful tool to assess the porosity characteristic in the concrete. An optimal threshold value was suggested, and the pores inside the concrete are identified successfully.
(2) At the initial exposure age, the porosity of deteriorated specimens increases slightly. Higher acidity of the solution leads to higher increase. The porosity has decreased 13.4% of the controlled specimen for specimens immersed in acid solutions with pH level of 1.5 up to 5 days. Porosity of specimen in the acid solution with pH level of 2.5 showed higher porosity up to 20 days, followed by the decrease in the later ages. The porosity has decreased 11.9% of the controlled specimen for 10 days, and the porosity decreased 51.8% after exposing for 40 days. The effect of the acid solution creates a more porous concrete microstructure in the concrete.
(3) Based on the probabilistic analysis, it is discovered that the distribution of the porosity in the concrete specimen sections obeys the normal distribution. Regardless of the pH level of the acid solution, the average porosity in the concrete specimen increase with the conditioning age linearly.
(4) The development of the porosity shows a good agreement with the results provided by the mass, strength analysis. The results obtained from macro, meso and micro tests are in good correlation with each other. Once the porosity inside the concrete is observed and determined, the mechanical property and durability of the concrete in-site can be evaluated.

Acknowledgements

This research was financially supported by the National Natural Science Foundation of China (Grant No. 51178069), National Natural Science Foundation of China (Grant No. 50708010), Program for New Century Excellent Talents in University (NCET-11-0860), and a Liaoning Provincial Fund for Distinguished Young Scholars.

References

[1] Gao J, Yu Z, Song L, Wang T, Wei S. Durability of concrete exposed to sulfate attack under flexural loading and drying–wetting cycles. Constr Build Mater 2013;39:33–8.
[2] Fan YF, Hu ZQ, Zhang YZ, Liu JL. Deterioration of compressive property of concrete under simulated acid rain environment. Constr Build Mater 2010;24:1975–83.
[3] Xie S, Qi L, Zhou D. Investigation of the effects of acid rain on the deterioration of cement concrete using accelerated tests established in laboratory. Atmos Environ 2004;38:4457–66.
[4] Tam WYV, Tam CM, Le KN. Removal of cement mortar remains from recycled aggregate using pre-soaking approaches. Resour Conserv Recycling 2007;50:82–101.
[5] Liu D, Windslow D. Pore structure of concrete. Publication FHWA/IN/JHRP-86/13. Joint Highway Research Project, Indiana Department of Transportation and Purdue University: Indiana (West Lafayette), 1986. http://dx.doi.org/10.5703/1288284314114.
[6] Chen MC, Wang K, Xie L. Deterioration mechanism of cementitious materials under acid rain attack. Eng Fail Anal 2013;27:272–85.
[7] Rimmelé G, Barlet-Gouédard V, Porcherie O, Goffé B, Brunet F. Heterogeneous porosity distribution in Portland cement exposed to CO_2-rich fluids. Cement Concrete Res 2008;38:1038–48.
[8] Cnudde V, Cwirzen A, Masschaele B, Jacobs PJS. Porosity and microstructure characterization of building stones and concretes. Eng Geol 2009;103:76–83.
[9] Chen H, Huang S, Tang C, Malek MA, Ean L. Effect of curing environments on strength, porosity and chloride ingress resistance of blast furnace slag cement concretes: a construction site study. Constr Build Mater 2012;35:1063–70.
[10] Abdelkader SM, Pozo ER, Terrades AM. Evolution of microstructure and mechanical behavior of concretes utilized in marine environments. Mater Des 2010;31:3412–8.
[11] Payan C, Garnier V, Moysan J. Effect of water saturation and porosity on the nonlinear elastic response of concrete. Cement Concrete Res 2010;40:473–6.
[12] Zhang S, Zhang M. Hydration of cement and pore structure of concrete cured in tropical environment. Cement Concrete Res 2006;36:1947–53.
[13] Duan P, Shui Z, Chen W, Shen C. Influence of metakaolin on pore structure-related properties and thermodynamic stability of hydrate phases of concrete in seawater environment. Constr Build Mater 2012;36:947–53.
[14] Mendes OA, Sanjayan JG, Gates WP, Collins F. The influence of water absorption and porosity on the deterioration of cement paste and concrete exposed to elevated temperatures, as in a fire event. Cement Concrete Comp 2012;34:1067–74.
[15] Chen H, Huang S, Tang C, Malek MA, Ean LW. Effect of curing environments on strength, porosity and chloride ingress resistance of blast furnace slag cement concretes: a construction site study. Constr Build Mater 2012;35:1063–70.
[16] JTGE30-2005. Test methods of cement and concrete for highway engineering. In: Chinese standard: Beijing, 2005.
[17] GB/T 50081–2002. Standard for test method of mechanical properties on ordinary concrete. In: Chinese standard: Beijing, 2003.
[18] Kanazu T, Matsumura T, Nishiuchi T, Yamamoto T. Effect of simulated acid rain on deterioration of concrete. Water Air Soil Pollut 2001;130(1-4 III):1481–6.
[19] Fan YF, Hu ZQ, Luan HY. Deterioration of tensile behavior of concrete exposed to artificial acid rain environment. Int J: Interact Multiscale Mech 2012;5(1):41–56.
[20] Kumara R, Bhattacharjeeb B. Porosity, pore size distribution and in situ strength of concrete. Cem Concr Res 2003;33:155–64.
[21] Benouis A, Grini A. Estimation of concrete's porosity by ultrasounds. Phys Proc 2011;21:53–8.
[22] Hernandez MG, Izquierdo MAG, Ibáñez A, Anaya JJ, Ullate LG. Porosity estimation of concrete by ultrasonic NDE. Ultrasonics 2003;38:531–6.
[23] Diamond S. Mercury porosimetry. an inappropriate method for the measurement of pore size distributions in cement-based materials – review. Cem Concr Res 2000;30:1517–25.
[24] Marchand J, Skalny JP. Materials science of concrete: sulfate attack mechanism, ed. USA: American Ceramic Society, 1999.
[25] Brown PW, Clifton JR. Mechanism of deterioration in cement- based materials and in lime mortar. Durability Build Mater 1988;5:409–20.
[26] Metha PK, Monteiro PJM. Concrete: microstructure, properties, and materials. New York: McGraw-Hill, 2006.
[27] Xie S, Zhou D, Yue Q. Research on mechanism of corrosion of non-metal building materials by acid deposition. Res Environ Sci 1998;11(2):15–7 [in Chinese].
[28] Zhang Y, Zhao Y, Fan Y. A Theoretical model for assessing elastic modulus of concrete corroded by acid rain. Eng Mech 2011;28(2):175–80 [in Chinese].